THE SOCIETY OF NAVAL ARCHITECTS AND MARINE ENGINEERS
One World Trade Center, Suite 1369, New York, N.Y. 10048

Papers to be presented at Extreme Loads Response Symposium
Arlington, VA, October 19–20, 1981

Strength of Ship Hull Girders under Moment, Shear and Torque

Alexis Ostapenko, Lehigh University, Bethlehem, PA

ABSTRACT

A method was developed for the determination of the ultimate strength of longitudinally stiffened ship hull girder segments of rectangular single-cell cross section, subjected to bending, shear and torsion. The principal features are: (1) Compatibility is enforced between individual nonlinear components of hull cross section; (2) Compression flange is treated as if it consisted of individual beam-columns each composed of plate-stiffener combination --- pre- and postbuckling, large deformations and plastification are taken into account; (3) Sides(webs) are analyzed by a multiple tension-field approach considering redistribution of normal and shearing stresses between plate subpanels. Comparison of the method with the results of three tests on a small hull girder specimen showed that the method is acceptably accurate for the loading case of moment and shear but needs additional work for the general loading case of moment, shear and torque.

NOMENCLATURE

A	area of cross section
a	length of test segment
b	width of test segment
b_c	spacing of longitudinal stiffeners in compression flange
C	proportionality factor between the cross-sectional shear and the load parameter W
C_1	bending moment-shear ratio
C_2	torque-shear ratio
d	depth of test segment
d_i	spacing of longitudinals in webs
E	Young's modulus of elasticity
e	eccentricity of the load
F_{bci}	buckling bending stress of the i-th web subpanel for pure bending
F_{cci}	buckling compressive stress of the i-th web subpanel for pure axial compression
F_{vci}	buckling shear stress for the i-th web subpanel for pure shear stress
F_y	yield stress
F_{ys}	static yield stress at zero strain rate
G	shear modulus
I	moment of inertia
L	computed length of the beam-column
M	bending moment
N	axial force, resulting from the stresses in the box section
P	axial force in the beam-column
P_u	ultimate axial force for the beam-column of length L_{max}
q	lateral loading per unit length of beam-column
r	radius of gyration = I/A
T	torque
t	plate thickness
V	shear force
V_{bi}	buckling strength of the i-th web subpanel
V_{tfi}	tension field strength of the i-th web subpanel

V_w shear force in web

V_{wu} ultimate shear capacity of web

W load parameter equivalent to a concentrated transverse load acting on a simply supported beam

W_u ultimate load parameter

α aspect ratio (=a/d)

α_{min} aspect ratio of the widest web subpanel ($=a/d_{imax}$)

Δ total axial shortening for the beam-column or compression flange

Δ_c axial shortening due to curvature

Δ_p axial shortening due to axial strain

Δ_{pu} axial shortening which exists under the ultimate force P_u

ε_{cr} plate buckling strain

ε_y yield strain

γ shearing deformation

γ_{ci} critical shearing deformation at point of buckling of the i-th subpanel

γ_{ui} ultimate shearing deformation of the i-th subpanel

σ_{ave} average stress for the plate of the compression flange

σ_{bci} bending stress which causes buckling of the i-th web subpanel when acting together with compression and shearing stresses

σ_{cr} plate buckling stress of the compression flange

σ_{cci} pure compression stress which causes buckling of the i-th web subpanel when acting together with shearing and bending stresses

σ_{ti} tension field stress at the ultimate condition for the i-th web subpanel

τ shearing stress

τ_{tfi} equivalent shearing stress in the i-th web subpanel due to tension field action

τ_{cci} shearing stress which causes buckling of the i-th web subpanel when acting together with compression and bending stresses

ϕ_o assumed mid-span curvature

INTRODUCTION

Background and Related Research

A need for developing a reliable method of evaluating the maximum strength of ship hulls has been becoming more and more important with the growing knowledge of ship loads. Although the traditional methods of ship design as evolved through the years of practical experience give adequately safe ship structures, it has been shown that the mechanism of failure is often very different from the mechanism predicted by these methods (1). Also, the rapid introduction of novel ship types (large tankers, container, LNG, special navy ships) required a more rational approach to ship design than the semi-empirical traditional methods.

Caldwell proposed to obtain the ultimate bending strength of a hull girder by assuming a fully plastified cross section. The postbuckling response of the plate components was to be incorporated by means of the effective width at the maximum plate capacity and the longitudinals were assumed not to buckle (2). The approach by Smith for the bending strength directly included the nonlinear response of the compression flange plating (3).

Much research has been conducted on the ultimate strength behavior of individual ship hull components: individual plates(4, 5, 6), stiffened plates and grillages(7, 8, 9, 10, 11, 12, 13, 14, 15, 16) and plate girders under shear and bending(17, 18, 19, 20, 21, 22, 23, 24, 25, 26, 27). However, knowledge of the behavior of individual components is not sufficient for accurately predicting the ultimate strength of a ship hull girder since the components reach their ultimate strength at different levels of deformation. Some segments may be already in the post-ultimate range of reduced capacity when others just attain their maximum strength. Also, the distribution of the internal forces to the components changes as the components become nonlinear.

Purpose and Scope

The main purpose of this research was to develop an analytical method for determining the ultimate strength of longitudinally and transversely stiffened box girders subjected to the combined effects of bending, shear and torque. Although a typical ship hull girder would normallly be subjected to

relatively small shear and torque values in comparison to the bending moment and, thus, the degradation of the moment capacity may not be of practically critical importance for such ships, box girders are used in a wider range of marine construction, such as in the cross structure of catamarans, special purpose ships, crane frames, etc. Therefore, it was considered important to develop a tool applicable to all box girder type structures under a general case of loading.

The basic individual components of a hull girder cross section are subjected primarily to uniform axial compression or tension with or without lateral pressure (bottom or deck plating), or to variable axial and shear forces (side plating). A typical cross section is shown in Fig. 1. In the

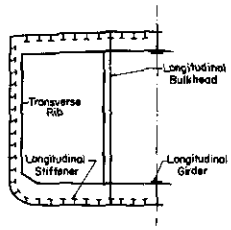

Fig. 1 Typical Mid-Ship Cross Section

development of the analytical model, a methodology was evolved for determining the relationship between the forces(moment, shear and torque) on the cross section and the axial deformation of the flange and side plating. Full advantage was taken of the research previously done on the strength of individual components. Of particular importance were the methods and computer programs developed at Lehigh University and elsewhere for the analysis of the ultimate strength of ship bottom plating(8, 10, 11, 12) and of plate girders(21, 22, 28). Three tests were conducted on a model hull girder in order to verify the soundness of some simplifying assumptions which had to be made in developing the theory and to point out the areas and considerations which should be included to make the theory more accurate.

METHOD OF ANALYSIS

Introduction

The thin-walled beam theory can be used for analyzing box girders when they behave linearly. However, this theory is no longer valid after the plate components buckle or behave nonlinearly.

The method proposed here considers the overall nonlinear behavior of a box section by taking into account the compatibility of deformations between the individual nonlinear components. Some of the novel features of the method are the consideration of strain reversal in the compression flange and the use of different materials for the plates of sides and flanges and the stiffeners.

The compression flange is treated as an assembly of beam-columns each analyzed by considering the pre- and postbuckling behavior of the plate and the large deformations of the plate-stiffener combination. The effect of residual stresses is taken into account. The tension flange is assumed to be linearly elastic-perfectly plastic. The side-plating is analyzed by considering the redistribution of shearing and axial forces between the plate subpanels, and the ultimate strength is obtained as the sum of the contributions of individual subpanels.

Analysis is performed on a hull girder segment defined as the longitudinal portion of the girder between two adjacent transverse stiffener rings or bulkheads. The forces on a segment (moment M, shear V and torque T) are expressed in terms of a load parameter W which is equivalent to a concentrated transverse load acting on a simply supported beam as shown in Fig. 2. These forces are assumed to be valid for the full length of the segment.

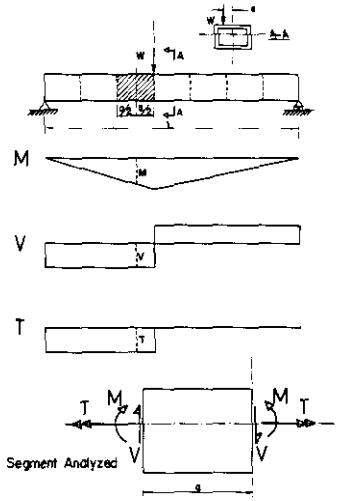

Fig. 2 Forces in Segment of Hull Girder Test Specimen

The following general assumptions are used to make the problem manageable:

1. Girder is straight and prismatic.

2. Cross section has a single cell rectangular shape and is symmetrical about its vertical centroidal axis.

3. A section plane before deformation remains plane after deformation. (This assumption was later modified to allow warping.)

4. Material has bilinear elastic-plastic stress-strain relationship. (However, nonlinear materials can be also considered by defining the stress-strain relationship with a series of points.)

5. Transverses are sufficiently rigid to provide unyielding support to the flange and web plating. Rotationally, this support can be pinned or fixed.

6. The effect of shear lag is negligible.

7. Transverse in-plane loads on the flanges and sides are negligible.

8. Stresses due to the deformation of the shape of the cross section are negligible.

Some additional assumptions are made in the discussion of particular items.

Forces on Components

In the linearly-elastic range of loading, the forces on the components of the cross section (flanges and sides) due to M, V, and T can be readily computed by using the ordinary beam theory. In this, essentially of torque T is carried by pure (St. Venant) torsion with a constant shear flow in all components even when the closed box section is restrained from warping (29).

After some plate components buckle, the mechanism of distribution of the component forces is modified by assuming that after buckling the side subpanels cannot carry any additional normal stresses and that shearing stresses are uniform in each particular subpanel but they have no effect on the ultimate strength of the flanges.

Before discussing the interaction between section components, the methods of analyzing the sides and flange plating are presented.

Behavior of Side Plating (Webs)

Sides (webs) of hull girders have the same basic geometry and are subjected to similar types of forces, bending and shear, as the webs of ordinary plate girders. Thus, it is prudent to take advantage of the research conducted on plate girders (17, 18, 19, 20, 21, 28, 30, 29). The only significant difference is in the relative size of the flanges and their ability to influence the postbuckling strength of the web plate since the thin flange plate of a hull girder provides little in-plane support to the web plate in comparison with the large flanges of a typical plate girder (28).

One of the simpler plate girder methods was selected and adjusted for the use in the box girder analysis (21, 30). Up to the buckling of one of the subpanels, the web is assumed to behave linearly with the shearing and normal stresses in a constant proportion. Then the postbuckling strength of this subpanel is assumed to develop independently from the behavior of other subpanels.

The maximum shear capacity of the whole web is given by the sum of the ultimate strengths of the component subpanels.

$$V_{wu} = \sum_{i=1}^{n} (V_{bi} + V_{tfi}) \qquad (1)$$

where

$V_{bi} = \tau_{ci} d_i t_w$ = buckling strength of the i-th subpanel (2)

$V_{tfi} = \tau_{tfi} d_i t_w$ = tension-field strength of the i-th subpanel (3)

In this analytical model the direct contribution of the flanges and longitudinal stiffeners to the total shear is neglected.

The critical shearing stress, τ_{ci}, of Eq. 2 for each i-th subpanel is found from the following interaction equation:

$$\left(\frac{\tau_{ci}}{F_{vci}}\right)^2 + \left(\frac{\sigma_{bci}}{F_{bci}}\right)^2 + \left(\frac{\sigma_{cci}}{F_{cci}}\right) \leq 1.0 \qquad (4)$$

Here the bending and normal stresses are in known proportions to the shearing stress. The reference buckling stresses F_{vci}, F_{bci}, and F_{cci} are computed by assuming the plate subpanels to be simply supported at all four edges and subjected to a respective stress acting alone (28). A transition between the yield level and the elastic range is taken into account.

The equivalent shearing stress of Eq. 3 reflects the postbuckling strength due to the tension field and is given by

$$\tau_{tfi} = \frac{\sigma_{ti}}{2\sqrt{2\ 1.6 + \alpha_{min}^2}} \qquad (5)$$

where

$$\sigma_{ti} = F_y - \sqrt{0.25(\sigma_{cci}-\sigma_{bci})^2 + 3\tau_{ci}} \quad (6)$$

is the tension field stress at the ultimate condition for the i-th subpanel, and

$$\alpha_{min}=a/d_{i\ max} \quad (7)$$

is the aspect ratio of the widest subpanel (28, 30).

Since the individual subpanels of the web in general have different depths d_i and are subjected to different combinations of bending and normal stresses, their buckling and the attainment of the ultimate condition do not occur simultaneously and are staggered in the course of the overall deformation of the web. The lower plot of Fig. 3 shows the shearing deformations of the three subpanels of a sample web shown in the upper sketch of the figure. The conditions of buckling and ultimate strength are labeled for subpanel 3, and they are seen to be at different levels of the overall shearing deformation than for the other two subpanels (21).

Deformation of each subpanel up to the point of buckling is linear and is defined by

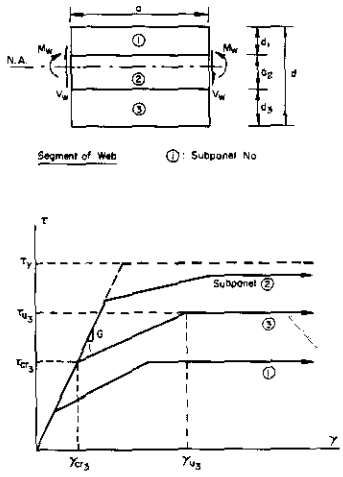

Fig. 3 τ-γ Relationship for Each Subpanel

$$\gamma_{ci}=\tau_{ri}/G \quad (8)$$

On the other hand, the postbuckling deformation cannot be accurately established. In Figure 3, it is approximated by a straight line connecting the buckling deformation with the ultimate deformation which is assumed to be reached when a diagonal fiber in the subpanel yields due to the racking deformation of the edge lines assumed to retain their original lengths (21). Thus,

$$\gamma_{ui} = \frac{F_y}{E}(\alpha_i + \frac{1}{\alpha_i}) \quad (9)$$

where

$$\alpha_i = a/d_i \quad (10)$$

The application of Eqs. 1, 2, and 3 at each of the kink points of the shear-deformation diagrams of Fig. 3 results in a relationship between the total shear V_w and the overall deformation for the whole web. In the process of computing this relationship it is important to keep in mind that, whereas the shear on a subpanel can increase after buckling, the normal stresses are assumed to remain constant and, thus, the additional moment corresponding to the increase in the total web shear must be redistributed to the flanges, the longitudinal web stiffeners and to the yet unbuckled web subpanels. With the assumption of "the plane section remaining plane", this redistribution process gives a corresponding relationship between the total shear V_w and moment M_w acting on the web and the normal strains at the top and bottom edges where the compatibility of strains is enforced between the webs and flanges.

In the present formulation, it is assumed that longitudinal stiffeners are linearly elastic up to yielding, but this assumption can be modified once the criteria for their premature failure or nonlinear behavior are established.

Behavior of Longitudinally Stiffened Compression Flange

Introduction. The compression flange of a hull girder section (the deck for the sagging and the bottom for the hogging moment) consists of a longitudinally stiffened plate subjected to axial compression and, for the bottom, lateral loading. The flange plating is assumed to be either simply supported or fixed at the transverses. The side edges (junctions to webs) are assumed to be free to rotate and displace in the plane of the plate (13). The nonlinearity of the axial behavior of such a plating arises from the welding residual stresses, buckling and postbuckling response of the plate components, initial imperfections and lateral loading. The method previously developed to consider these effects by replacing the analysis of a longitudinally stiffened plate panel with a large-deflection analysis of a beam-column was adapted for the present research (10, 11).

The simplifying assumptions of the method are the following:

1. The plate is very flexible in comparison with the relatively large longitudinals and therefore the interaction between the longitudinals through the plate may be neglected. Then, each longitudinal with its tributary portion of the plate may be considered as an independent substitute beam-column subjected to axial and lateral loads.

2. The response of the plate component of the beam-column cross section corresponds to the behavior of a long plate with the width equal to the spacing of the longitudinals. The side edges are assumed to be simply supported, but they must remain straight although they may have in-plane motion.

3. The effect of lateral loading on the plate behavior is negligible since it has been found to have little effect on the buckling and postbuckling behavior(10), and the bending stresses (in the plate spanning between longitudinals) may be treated as a tertiary condition and checked separately. Then, the distributed lateral loading is applied as a line load q on the beam-column as shown in Fig. 4.

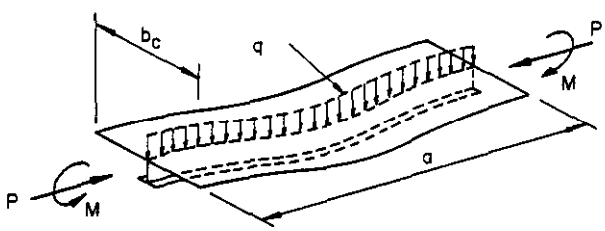

Fig. 4 Beam-Column Idealization

Since the original computer program gave only the length of a pin- or fixed-ended beam-column which was in equilibrium under the given axial and lateral loads for an assumed mid-span curvature, several supplementary operations had to be developed to obtain a complete axial load versus deformation relationship for a zero lateral loading and a specified length. Principal operations of the final program are briefly described here.

Behavior of Plate under Compression. The axial behavior of a stiffened plate under compression is described by a relationship between the average stress and the overall strain which is also the strain at the edges. Such a relationship can be supplied to the program by a series of points obtained, for example, from a test, or by a computational procedure. In the computational procedure used, it is assumed that the plate is perfectly flat and the effects of the shearing stresses on the axial buckling stress and the postbuckling behavior are negligible (31).

The three ranges of the plate response when the plate is subject to buckling are shown in Fig. 5 on the average stress vs. strain curve.

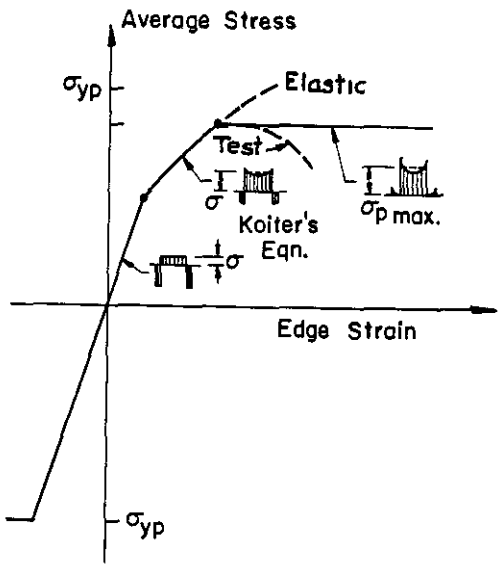

Fig. 5 Average Stress vs. Edge Strain Relationship for Plates under Compression with Welding Residual Stresses

1. The linearly (or nonlinearly) elastic prebuckling range. The stress is uniform and the end of the range is limited by the buckling stress (the buckling coefficient is conservatively taken to be k= 4.0).

2. Elastic postbuckling range. The elastic postbuckling relationship is described by the Koiter equation which gives the average stress in terms of the overall (edge) strain (4).

$$\frac{\sigma_{ave}}{\sigma_{cr}} = 1.2\left(\frac{\varepsilon}{\varepsilon_{cr}}\right)^{0.6} - 0.65\left(\frac{\varepsilon}{\varepsilon_{cr}}\right)^{0.2} + 0.45\left(\frac{\varepsilon}{\varepsilon_{cr}}\right)^{-0.2} \quad (11)$$

The stress pattern is nonuniform, and the average stress vs. strain relationship is noticeably flatter than the material stress-strain curve.

3. Ultimate stress condition is assumed to be reached when the maximum (edge) stress of the nonuniform

pattern reaches yield stress level. This assumption has been confirmed by numerous tests and some theoretical analyses (6, 7, 10). Compression of the plate beyond this point generally shows a reduction of the average stress as indicated in Fig. 5 by the curve portion labeled "True" (6, 7). However, sample computations have demonstrated that in stiffened plating of the proportions typical for ship structures, ultimate strength of the plating is reached at the plate strains which do not significantly exceed the ultimate strain and, when they do, the effect is negligible. It is thus reasonable to assume that, as shown in Fig. 5, the average stress remains constant for deformations beyond the ultimate condition (10).

The effect of the welding residual stresses was included in this method (10).

Beam-Column Analysis. The beam-column to be analyzed is shown in Fig. 4. It is subjected to an axial load P, end moments M and a line loading q. The cross section consists of the plate with the stress-strain characteristics established above and the longitudinal stiffener with a stress-strain response given by the material.

The purpose of the analysis is to establish the relationship between the axial load and axial deformation. The process requires several interdependent steps.

The first step is to develop a series of relationships between the mid-span curvature and the length of the beam-column of the given cross section when the line load is kept constant and different axial load is applied. A previously developed computer program is used for this purpose (10, 11, 32, 33). The resultant curves are shown in Fig. 6a. Each time an iterative numerical integration is involved.

The next step is to transform the length L vs. ϕ_o mid-span curvature relationships into the length vs. axial shortening relationships by utilizing the length shortenings computed in the first step. The resultant L vs. Δ curves are shown for different axial loads P in Fig. 6b.

Since the given beam-column has a specific length a, the relationship between P and Δ is obtained by passing a horizontal line in Fig. 6b for L=a and taking the Δ-values corresponding to each value of P. The results are then combined into a P vs. Δ curve valid for

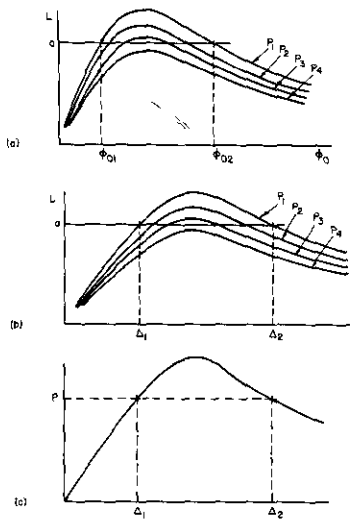

Fig. 6 Procedure of Obtaining P vs. Relationship for Given q

a specified line loading q and length L=a as shown in Fig. 6c. The peak of the curve gives the ultimate axial strength of the beam-column.

Effect of Strain Reversal. A special correction for the effect of strain reversal had to be made in the post-ultimate range of the P-Δ relationship. The need for this arose from the fact that the procedure described above for obtaining the L vs. ϕ_o and ΔP vs. curves is based on formulating an equilibrium condition on a member deformed to the configuration considered. This is equivalent to obtaining each point of the P-Δ curve as if the path of deformation followed a straight line from the origin as indicated by the dashed line in Fig. 7. Whereas the pre-ultimate range of the P-Δ curve which for an increasing value of P is not affected by this procedure, the post-ultimate range becomes very distorted. This is shown in Fig. 7 by the dotted z-shaped curve defined by

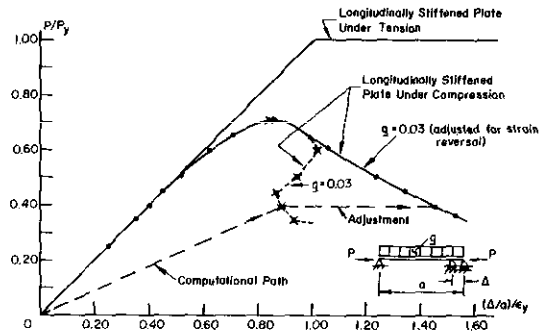

Fig. 7 Load vs. Axial Shortening Adjusted for Strain Reversal

crosses. In this case, the nonlinear and plastic deformations which had taken place under the higher past load and subsequent elastic relaxation are not taken into account.

In order to correct the anomaly of the reduction of the deformation indicated by the dashed curve, the true deformation path including the strain reversal resulting from the drop in the axial load in the post-ultimate range was approximated by modifying the Δ-value as follows. Since the total shortening consists of two parts,

$$\Delta = \Delta_p + \Delta_c \qquad (12)$$

Δ_p= axial shortening due to axial strain (effect on P)

Δ_c= axial shortening due to curvature,

it was assumed that in the post-ultimate range Δ_p remains constant and equal to Δ_{pu}, that is, the value which existed under the ultimate load P_u (at the peak). Then, the shortening in the post-ultimate range becomes

$$\Delta = \Delta_{pu} + \Delta_c \qquad (13)$$

The result of this adjustment is shown in Fig. 7.

Axial Behavior. The procedure described above requires that the lateral line loading q be non-zero and thus the procedure is not directly applicable to the analysis of ship deck plating. To obtain the pure axial load vs. shortening behavior, a set of P vs. Δ relationships are computed for decreasing values of q and the P-values for q = 0 are extrapolated.

Two examples of graphical extrapolation are shown in Fig. 8 for the ultimate capacity of the compression flange of the test specimen. The top plot is for the original design dimensions and the nominal yield stress. The bottom plot is for the dimensions

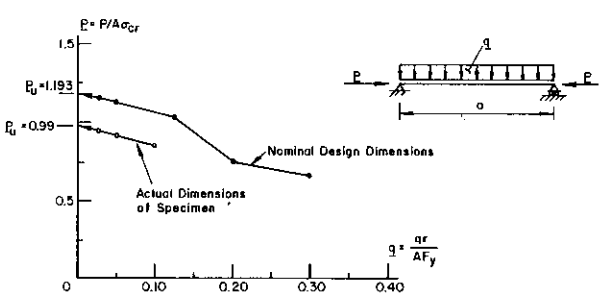

Fig. 8 Extrapolation of Pure Axial Strength from Beam-Column Strengths

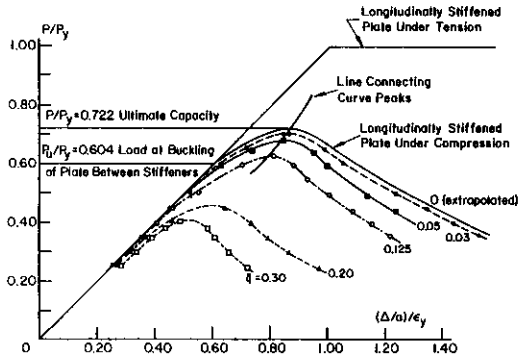

Fig. 9 Load vs. Shortening of Stiffened Plate under Axial Compression and Normal Loading

and the yield stress as they were measured in the fabricated specimen. Another example is given in Fig. 9 where the complete P vs. Δ curve with a number of initial curves for various values of q is shown. Usually three values of q between 0.03 and 0.10 were sufficient.

For comparison, the response of a tension flange, corresponding to the material stress-strain diagram, is also shown in Fig. 9. Also, for greater convenience, the axial load is nondimensionalized to $P/P_y = P/(AF_y)$ and the axial shortening to $\Delta/a\,\varepsilon_y$.

Consideration of Initial Imperfections. Initial deflections due to fabrication were not considered in the procedure described above. However, a modification can be readily made by transforming the initial deflection patterns into a curvature diagram and then adding the corresponding curvature values at each segment in the integration process. Since the integration length L may be longer than the actual length of the beam-column a, the initial curvature diagram should be extended by, for example, making it constant and equal to the value of curvature at the end or to zero.

Behavior and Ultimate Strength of Hull Girder Segment

Once the load-deformation behavior of the individual components is defined, the analysis of the entire hull girder segment proceeds by enforcing the compatibility between these components as the load is incremented. The following load-deformation relationships of the components are involved:

- τ vs. γ relationships for the individual subpanels of the sides (webs) (Fig. 3).

- P/P_y vs. $(\Delta/a)/\varepsilon_y$ relationship for the longitudinals of the compression flange, each with its share of the plate (Fig.9).

- σ vs. ε relationship (material curve) for the tension flange, and the stiffeners and the unbuckled subpanels of the webs.

The internal forces acting on the mid-segment section (moment, shear and torque) are related to loading parameter W as shown in Fig. 2 and can be expressed by the following equations:

$$V = C\ W \tag{14}$$

$$M = C_1\ d\ V = C\ C_1\ d\ W \tag{15}$$

$$T = C_2\ d\ V = C\ C_2\ d\ W \tag{16}$$

where: C= proportionality factor between the cross-section shear and W,

C_1 moment-shear ratio = M/(Vd),

C_2 torque-shear ratio = T/(Vd), and

d = depth of the cross section

The deformation parameter to be used against W in the computer program was chosen to be the average strain in the junction line between the web and the compression flange. This strain corresponds to the average shortening of the compression flange, Δ/a. An example of the resultant curve for the load-deformation relationship is shown in Fig. 10. This curve is for Test 1 but using the initial design dimensions and a somewhat different test arrangement than in the actual test.

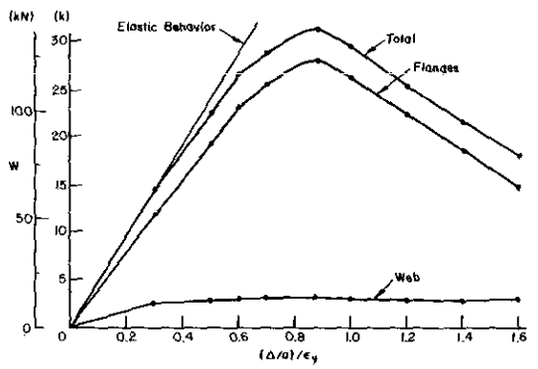

Fig. 10 Load Distribution between Webs and Flanges for Box Section under Shear and Bending

The procedure for obtaining the W vs. $(\Delta/a)/\varepsilon_y$ relationship is according to the following basic steps:

1. An initial value of the web (side)-to-compression flange junction strain is assumed and the strain at the other edge of the web is iterated until the total axial force on the cross section is equal to zero (N=0). Since the cross section is assumed to remain plane, the strain distribution at each iteration is used for computing the normal stresses and then the resultant axial force and the bending moment. Once the axial force is equal to zero (N=0), the relationships of Eqs. 14 to 16 provide a means for computing W, V, and T and the resultant shearing stresses. If there is no buckling in the web subpanels, the assumed junction strain and the W-value provide one point for the curve. Then, the junction strain is incremented and the process is repeated for additional points.

2. If the shearing stress in a particular web subpanel becomes higher than the critical (or ultimate) value indicated in Fig. 3, the junction strain must be reduced and the procedure repeated until a value acceptably close to the critical (or ultimate) shearing stress is found. At each iteration after subpanel buckling, the redistribution of shearing stresses between individual subpanels takes place to maintain shear deformation compatibility as shown by the curves in Fig. 3. Thus, the operations of this step must be repeated at each kink of these curves.

3. As the junction strain values are increased and the corresponding values of W are computed, a complete W vs. junction strain is obtained, including the pre- and postultimate ranges.

In the example of Fig. 10, the junction strain is non-dimensionalized with respect to the yield strain. Contributions of the webs and flanges to the total load are shown by separate curves. The share for each was taken to be proportional to the percentage of the moment carried by the respective component.

Modified Computer Program

The computer program, based on the procedure described above, correlated well with the test result on the hull-girder segment subjected to shear and bending (Test 1), but it was too optimistic when torque was also applied (Tests 2 and 3).

The computer program was then modified not to require that the section remain plane and two corner strains were introduced into the iterative process with two other corner strains gradually incremented. The variation of the axial deformations (axial strain) across the width of each component (flange or web) was assumed to be linear. Thus, each

longitudinal of the compression flange made a different contribution in accordance with the P vs. Δ relationship. The criteria used for the convergence of the two iterated strains were that the axial force and the moment about the vertical axis be equal to zero (N=0 and M_y= 0).

The results from the modified program give a better correlation with tests, but the program needs further work (as of May 1981).

TEST SPECIMEN

A test specimen had been designed to conduct three tests under different combinations of moment, shear and torque. For each test, a particular segment was tested to failure while the other two segments were reinforced. Figure 11 shows the test arrangement for each of the tests and the corresponding combinations of moment, shear and torque defined in terms of the jack load W.

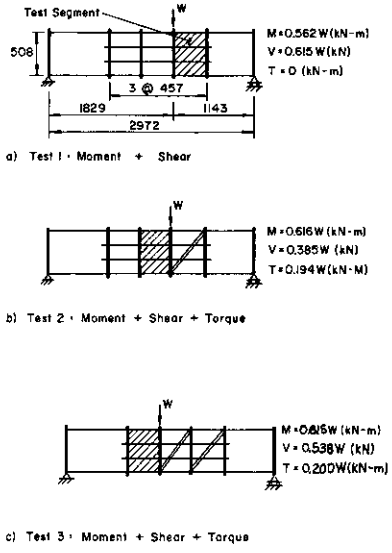

Fig. 11 Test Segments and Forces

Test 1(Fig 11a) : Bending moment and shear.

Test 2(Fig. 11b): Bending moment shear and torque.

Test 3(Fig. 11c): Another combination of bending moment, shear and torque.

The scantlings of the test specimen were selected to model the relative proportions of the components of a typical hull girder. Two views and the principal cross sections are shown in

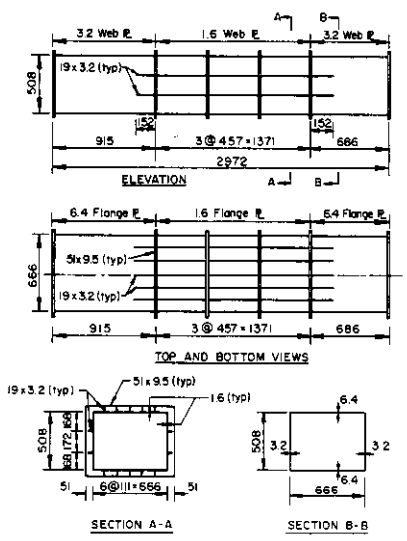

Fig. 12 Test Specimen Scantlings

Fig. 12. The spacing of the longitudinals and the thickness of the plate in the test portions were selected so that plate instability would occur before reaching the ultimate capacity. The scantlings of the fabricated specimen were slightly different than the design scantlings shown in Fig. 12. The most significant change was in the plate thickness from 1.59 mm (1/16 in.) to 1.85 mm (0.073 in.). The test specimen was fabricated from ASTM A36 steel plate with a nominal yield stress of 250 MPa (36 ksi) and the actual static yield stress in the longitudinal direction of 237 MPa (34.34 ksi) and the dynamic yield stress at the strain rate of 1042 μm/m/sec (ASTM strain rate) of 280 MPa (40.55ksi) (34).

Although residual stresses due to the yielding process were not measured, some reasonable levels of intensity were assumed in the computer analysis.

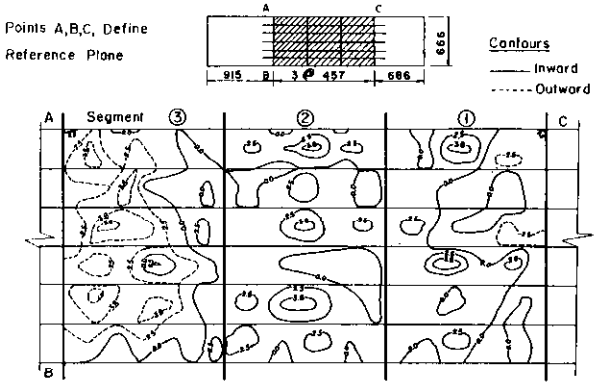

Fig. 13 Initial Imperfections in the Compression Flange (all dimensions in mm)

Initial deflections were measured for the plates of the webs and the compression flange. For the webs, the maximum offsets were of the order of ±4.8 mm (0.19 in.), i.e., approximately 2.6 times the plate thickness. Initial imperfections of the compression flange are shown in Fig. 13 by a contour map. Most of the offsets are in the range of ±2.54 mm (±0.1 in.) with the maximum values of the order of ±5.08mm (±0.2 in.), i.e., 2.7 times the plate thickness.

TEST PROCEDURE AND RESULTS

The test setup is shown in Fig. 14. The specimen is positioned on two support pedestals, and a concentrated load is applied by means of a jack attached to a transverse beam of the test frame. The load is transmitted to the test specimen by a spreader beam, set transversely on two plates welded to the transverse stiffeners of the webs, as shown in Section A-A. For Test 1, the cross section was loaded symmetrically (Section A-A) and for Tests 2 and 3 with an eccentricity.

There were three points of support for the specimen. The X-Y roller bearing at one end consisted of an arrangement of two mutually perpendicular rollers separated by a plate so that rotation and translation were possible in the longitudinal and transverse directions. The other end had two X-roller bearings, one on each side of the cross section, which permitted free rotation. In Tests 2 and 3, one of these two supports was also anchored down to prevent uplift of the support due to torsion.

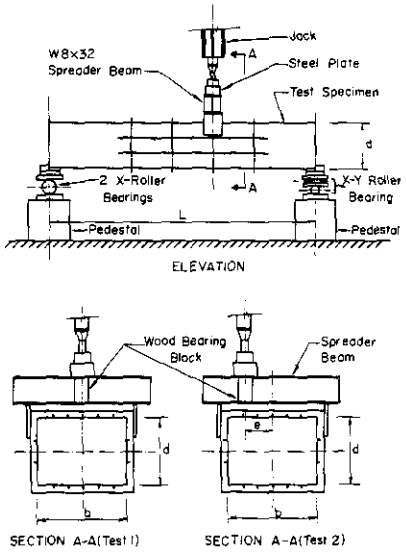

Fig. 14 Test Setup

To accomplish several tests on the same specimen, the segments adjacent to the test segment were reinforced by small steel bars cee-clamped to the longitudinal stiffeners, corner angles at the web-to-compression flange junctions and by pieces of wood on the compression flange. For the yet untested segments these reinforcements were tightly wedged between the transverses. For the already tested segments, the reinforcement bars and the corner angles were tack welded to the compression flange, and the webs were reinforced with steel bars welded to the transverse stiffeners in the direction of the tension diagonal.

Instrumentation

The instrumentation consisted of both mechanical dial gages and electric resistance strain gages. The dial gages were used to measure the vertical deflections of the specimen along both webs. The approximately fifty linear and three-branch-rosette strain gages provided information about the stress distribution over the cross section and about the tension field pattern which developed after theoretical buckling of the webs.

Diagonal deformations of the sides of the tested segments were measured by means of a portable variable-length extensometer. This extensometer was also used at other points to measure the variation of the segment length between transverse stiffeners. Distortion of the cross section at the ends of the test segment was measured by means of electrical extensometers placed diagonally from corner to corner (Test 3).

Test Results

In all three tests, the ultimate capacity was limited by the failure of the compression flange characterized by large out-of-plane deformations as shown, for example, in Fig. 15 for Test 1.

Vertical deflection of the heavier loaded web at the transverse under the load was used as the principal indicator of the overall deformations of the tested segment. Figures 16, 17, and 18 show the plots of the applied load W vs. this deflection, respectively, for Tests 1, 2 and 3. The points plotted near the ultimate load and in the post-ultimate range correspond to the maximum load recorded for that deflection and, thus, they were affected by the loading rate (actually, the straining rate). The zig-zag pattern in the right-hand portion of Fig. 18 illustrates the

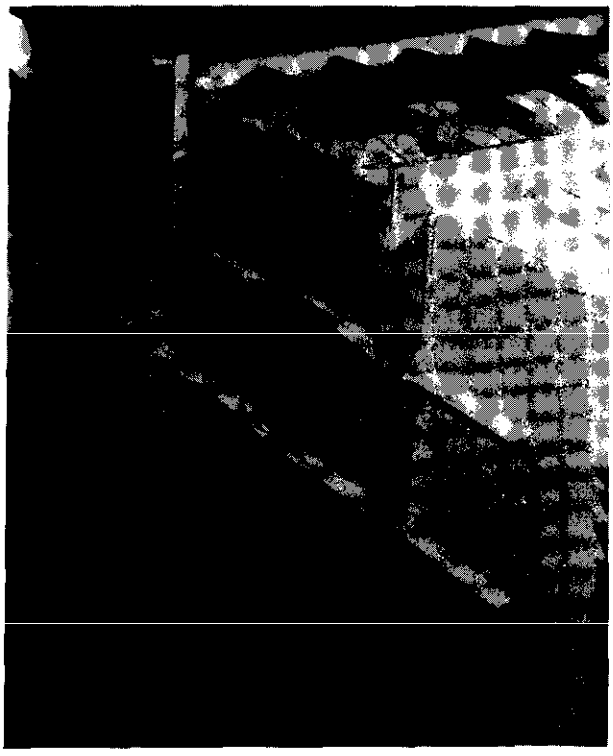

Fig. 15 Deformation of Compression Flange and Web 1 (Test 1)

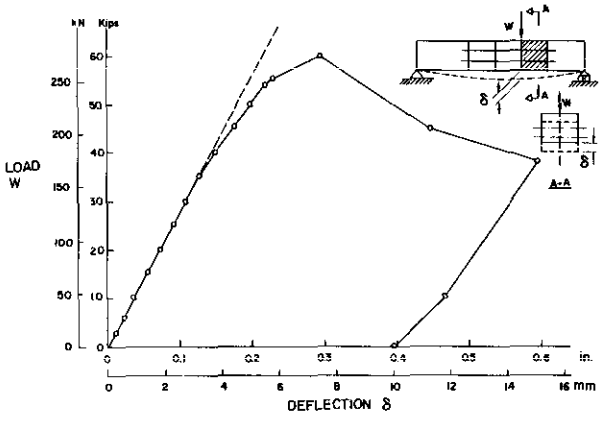

Fig. 16 Load vs. Deflection Curve for Test 1

reduction of the maximum load to the stabilized load after closing the valve of the testing machine.

The overall behavior of the test segment, as shown in Figures 16, 17 and 18, is characterized for all three tests by the following four portions:

1. Linear; up to 0.5-0.6 of W_u (ultimate load).

2. Gradually curving; up to the ultimate load W_u. The deviation of the curve from linearity appeared to be mainly due to the increase of the out-of-plane deflections of the compression flange and the upper web subpanels and due to local yielding.

3. Post-ultimate drop-down portion. After reaching the ultimate capacity, the load suddenly (Test 1), or gradually (Tests 2, and 3), dropped and then stabilized. When the machine valve was opened again, the load climbed somewhat and then dropped further to a lower stable level.

4. Unloading portion. After obtaining the post-ultimate range the girder was unloaded to zero in two or more steps.

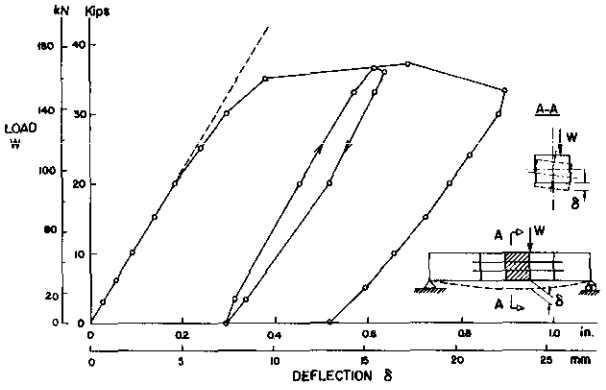

Fig. 17 Load vs. Deflection Curve for Test 2

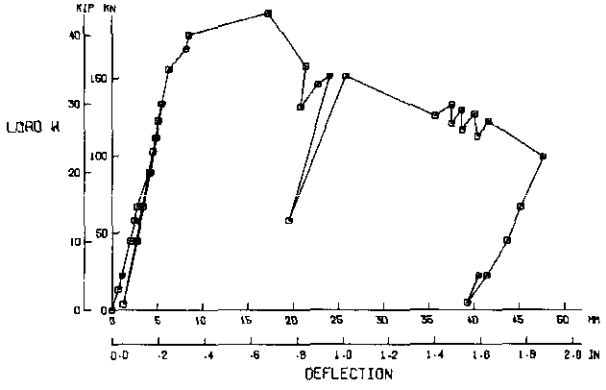

Fig. 18 Load vs. Deflection Curve for Test 3

Diagonal Deformations of the Web

A good representation of the behavior of a test segment is given by a plot of deformations (changes in length) of the compression and tension diagonals of the web versus the applied load W. For example, Fig. 19 shows the

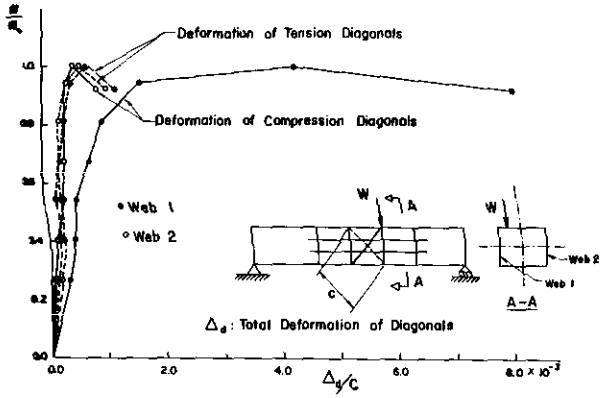

Fig. 19 Diagonal Deformations of Webs 1 and 2 (Test 2)

relative diagonal deformations, respectively shortening and elongation, of the compression and tension diagonals of the two webs of Segment 2 (Test 2). Other segments behaved similarly.

Because of the load eccentricity, one web (Web 1) was subjected to a higher shear than the other (Web 2), and, therefore, the deformations of the two webs are noticeably different. The response of the tension and compression diagonals for Web 2 (smaller shear) and the tension diagonal for Web 1 are essentially linear up to 0.95 W_u. A sudden change in the slope occurs at this load before the ultimate load is reached. Deformation of the compression diagonal of Web 1 was much more pronounced. Although the curve is essentially linear up to 0.54 W_u, the slope is noticeably flatter than for the other diagonals, then, it reduces further and after 0.95 W_u becomes almost horizontal until the curve reaches the ultimate load W_u. Actually, the load at which the response of the compression diagonal of Web 1 becomes nonlinear corresponds to the beginning of the nonlinear portion of the load-deflection curve of Fig. 17.

The larger deformation of the compression diagonal of Web 1 than of the tension diagonal demonstrates the extent of the overall shearing distortion of the panel caused by subpanel buckling and the shortening of the compression flange on this side. For Web 2, the deformations of the tension and compression diagonals are approximately the same indicating a relatively linear shearing deformation.

Strain Distribution in Cross Section

Strain readings provided a means of determining stresses in the tested segment and comparing these with the computed stresses. However, since the gages were placed only on the outside surface and the plate components had impractically large initial deflections, the readings could not be considered to give accurate values of axial cross-sectional stresses, especially in the post-buckling range. Still, the distribution of the measured strains in the cross section gave a good indication of the behavior of the tested segments.

Probably the most significant is a comparison between the strain distributions in a segment subjected to moment and shear (Test1) and in a segment subjected to moment, shear and torque (Tests 2 and 3). Figure 20 shows the strains across the half-width of the compression flange for Test 1 (the other half is approximately symmetrical). Although there is a significant reduction of strains (and, thus, stresses) away from the edge, especially at higher load values, the middle

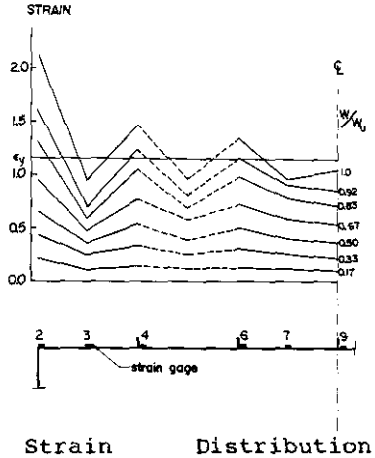

Fig. 20 Strain Distribution at Mid-Length of Compression Flange (Test 1)

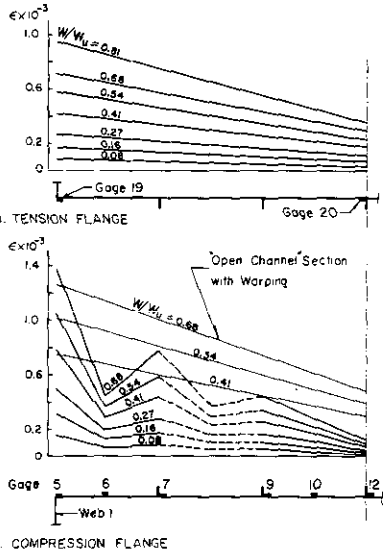

Fig. 21 Strain Distributions in Flanges for Half-Width (Test 2)

portion has a relatively uniform distribution. In contrast to this, the strain distribution in Fig. 21, (Test 2) is basically linear except for the variation between subpanels and longitudinals and the increase at the edge, and is thus analogous to the theoretical strains given by the thin lines for an "open channel" section. This means that there was a gradual transition from a closed to an open section as the heavier loaded web (Web 1) was weakening while the web subpanels were going into the post-buckling range.

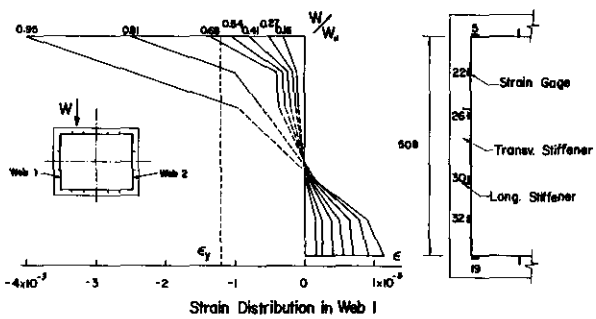

Fig. 22 Strain Distribution in Web 1 (Test 2)

Figure 22 shows the strain distribution across Web 1 of Segment 2. The distribution patterns for the individual loads are very irregular and can hardly be considered to support the "plane section remaining plane" hypotheses. However, except for the last two load increments, the neutral axis remained at essentially the same location, although below the mid-depth point. This indicates that the overall response of the cross section was essentially linearly elastic with the compression flange being "weaker" than the tension flange. The downward shift of the neutral axis for the loads over 0.68 W_u was mainly caused by the progressive failure of the compression flange and of the top web subpanel.

COMPARISON OF ANALYTICAL AND EXPERIMENTAL RESULTS

The tested girder segments were analyzed by the method described above.

Since the three segments had the same dimensions, the response of the longitudinals in the compression flange to axial force was the same. Thus, the difference from test to test was only in the moment-shear-torque combinations as shown in Fig. 11. Table 1 lists these combinations in terms of the non-dimensionalized parameters C, C_1, and C_2 (see Eqs. 14, 15, and 16). Analysis of the test segments or the ultimate load by using the proposed method gave the values shown in Table 1. The experimental values are also listed in the table.

Table I. Specimen Parameters and Ultimate Loads

Test	1	2	3
Shear/W = C	0.615	0.385	0.538
M/Wd = C_1	1.106	1.213	1.211
T/Wd = C_2	0	0.382	0.393
Load			
W_u (kN)			
W_{exp} (kN)	266.9	164.6	192.4
W_{theo} (kN)	306.9	280.2	276.9
W_{theo}/W_{exp}	1.15	1.70	1.44

The ratios of the theoretical and experimental ultimate loads, W_{theo}/W_{exp} given in the last line of the table show that the theory is only 15% too optimistic for the segment not subjected to torque (Test 1) but 70% and 44% for the segments which are subjected to torque (Tests 2 and 3, respectively).

The computed load vs. junction strain relationships for Tests 1 and 2 are plotted in Fig. 23. Both curves are linear up to the first kink which corresponds to the buckling of the top web subpanel (Webs 1 and 2 for Test 1 and Web 1 for Test 2). There is one more kink in each curve before the ultimate load is reached, and it reflects the buckling of the middle web subpanel. The post-ultimate range exhibits a rapid reduction in strength. It is noteworthy that the ultimate strength developed at approximately 0.89 ε_y on the abscissa, that is, before the junction had an average strain equal to the yield strain. However, this prediction could not be checked by experimental results since the strain gages measured not the average but only the local strains at a few locations.

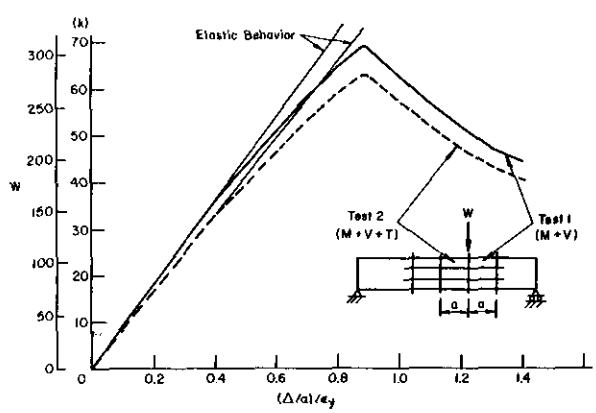

Fig. 23 Load vs. Average Strain in Flange-Web Junction for Tests 1 and 2

All three tests confirmed qualitatively the analytical prediction that the strength of the box section was limited by the capacity of the compression flange.

The substantially lower experimental loads for Tests 2 and 3 could be only partially explained by the measurements and observations. Apparently, the most significant weakening effect was made by the transformation (from the analytical point of view) of the closed box section into a partially open channel-type section with the corresponding shift of the shear center. This effect would be caused by the "softening" of the heavier loaded web as its subpanels went into the postbuckling range. Such transformation would not only force the section to carry an increasing portion of the torque by warping torsion (vs. the pure St. Venant torsion) but also, as mentioned above, amplify the torque itself as the shear center shifted away from the weaker web (Web 1) toward the more rigid web (Web 2). The nonuniform distribution of the strains in Fig. 21 confirms this conclusion. A similar distribution was also found for Test 3.

After the computer program was modified to allow non-planar deformation of the cross section, analysis of the ultimate condition of Test 3 was performed by inputting the actual experimentally measured strains at three corners and iterating the fourth strain to converge the total axial load to zero (N=0). The ultimate load was computed to be W_{theo} = 250.1 kN, that is, 1.30 W_{exp} rather than 1.40 W_{exp}, and, with some additional assumptions (including the setting of the compressive residual stress equal to 20% of the yield stress), W_{theo} = 214.3 kN, that is, 1.14 W_{exp} which gives only 14% deviation.

It appears, thus, that a modification of the program to perform iteration of the strains at two corners and imposing the requirement that N=0 and M_y = 0 should lead to a workable program. Such a program has not been properly tested yet (May 1981).

SUMMARY, CONCLUSIONS AND RECOMMENDATIONS

Summary

A theoretical and experimental study was performed on the pre- and postultimate behavior of longitudinally and transversely stiffened box girders of the scantlings typical for ship hulls. Two loading conditions were considered: (1) moment and shear, and (2) moment, shear and torsion. Three tests were conducted on a hull girder specimen to verify the analytical method.

The principal feature of the analytical method was the consideration of continuous interaction between the components of a hull girder cross section through the compatibility of axial strains at the junction lines between the deck, side and bottom platings. This was needed for the following reasons:

1. The danger of computing the maximum strength of a hull cross section by adding the maximum strengths of the individual components rests on the fact that the segments reach their maximum strengths at different levels of deformation. Thus, some segments may be already in the post-ultimate range of reduced capacity when some others just attain their maximum strength.

2. Redistribution of internal forces, specifically, of the bending moment between the webs and flanges could be considered by maintaining compatibility of strains at the junction lines and requiring that "plane sections remain plane" or that the section may warp, but the strains vary linearly across the width of each component.

The behavior and ultimate strength of individual components of the cross section was established by adapting and extending available methods. The compression flange was analyzed as if it was composed of a series of substitute beam-columns each consisting of a stiffener and a plate and subjected to axial and lateral loads. Buckling and post-buckling response of the plate, plastification and large deformations were considered. The webs were analyzed by using an ultimate strength theory previously developed for longitudinally stiffened plate and box girders.

The three tests conducted on separate segments of the hull girder specimen led to the following observations:

Test 1 (moment and shear): (1) The experimental ultimate load was 15% below the theoretical load; (2) The experimental stress distribution in the compression flange agreed well with the theoretical up to 50% of the ultimate load. Then, there was a predictable deviation, with the stresses at the web-flange junction becoming significantly higher than in the middle portion of the flange.

Tests 2 and 3 (moment, shear and torque): (1) The experimental ultimate load was 70 and 44% below the predicted load, respectively for Tests 2 and 3. (2) Contrary to the analytical prediction, the stresses measured in the tension and compression flanges were not distributed uniformly or symmetrically. Apparently, the rigidity of the web subjected to a greater shear was deteriorating much faster than anticipated. The consequent redistribution of internal forces made the cross section to behave as if it was gradually transformed from a closed box to an open channel section.

Conclusions

Comparison of the theoretical and experimental results showed that in the case when only moment and shear are acting on the girder segment (Test 1), the original analytical method was acceptably accurate although it was somewhat optimistic.

However, the method was found to give significantly higher ultimate capacity when the girder segment was subjected to the general loading of moment, shear and torque (Tests 2 and 3). Although the values of shear and torque used in this analysis were relatively higher than those encountered in ordinary ship hulls, the method is important since box girders are used in a wider range of marine structures, for example, in the cross structure of catamarans.

Recommendations for Future Research.

In order to meet the original objective of developing a reliable method for hull girders under moment, shear and torque the following improvements are recommended:

1. Tests on hull girder segments of larger dimensions, so that the initial imperfections would be in the relative practical range.
2. Inclusion of the effect of shearing stresses on the strength of flanges, especially of the compression flange.
3. Inclusion of the effect of shear lag.
4. Refinement of the strength formulation for the webs.
5. Inclusion of the effect of warping by the consideration of nonuniform but linearly varying axial shortening (or elongation) across the width of the flanges and sides (current work).
6. Consideration of the deformation of the shape of the cross section when transverse rings (diaphragms, transverse bulkheads) are not sufficiently rigid.

ACKNOWLEDGEMENTS

The author is grateful to the Maritime Administration for sponsoring this research under the MARAD University Research Program Contract Nos. MA-79-SAC-B0019 and MA-80-SAC-01081. The help by Mr. F. Seibold, Program Manager, and Dr. W. M. Maclean, Technical Coordinator, is appreciated.

Mr. A. Vaucher was the principal co-worker in this research and he was instrumental in developing the test arrangement and in conducting the first two tests, as well as, in their analysis and in the preparation of the pertinent drawings. Mr. M. F. Salley conducted the third test.

Thanks are also due to Messrs. Y. F. Chen and P. A. Ostapenko who assisted in the technical production of this paper.

REFERENCES

1. J. Vasta, "Lessons Learned from Full Scale Structural Tests," Transaction SNAME, Vol. 66, p. 165, 1958.
2. J. B. Caldwell, " Ultimate Longitudinal Strength," Proceedings of the Royal Institution of Naval Architects, Vol. 107, London, 1965.
3. C. S. Smith, "Influence of Local Compressive Failure on Ultimate Longitudinal Strength of a Ship's Hull," PRADS - International Symposium on Practical Design in Shipbuilding, Tokyo, 1977.
4. W.T.Koiter, "The Effective Width of Flat Plates for Various Longitudinal Edge Conditions at Loads Far Beyond Buckling Load,"National Luchtvaartlaboratorium, Netherlands, Rep. S287 (in Dutch), 1943.
5. T.T.Lee, "Elastic-Plastic Analysis of Simply Supported RectangularPlates Under Combined Axial and Lateral Loading," Fritz

Engineering Laboratory Report No. 248.7, Lehigh University, 1961.

6. K.E. Moxham and C.D. Bradfield, "The Strength of Welded Steel Plates under Inplane Compression," University of Cambridge, Department of Engineering, Technical Report No. CUED/C-Struct/TR.65, 1977.
7. J. Dwight, "Collapse of Steel Compression Panels," Trans. Developments in Bridge Design and Construction, University College, Cardiff, 1971.
8. J. Kondo, "Ultimate Strength of Longitudinally Stiffened Plate Panels Subjected to Combined Axial and Lateral Loading," Fritz Engineering Laboratory Report No. 248.13, Lehigh University, 1965.
9. H. Becker and A. Colao, "Compressive Strength of Ship Hull Girders," (Part III, "Theory and Additional Experiments"), SSC No. 267, Ship Structure Committee, Washington, 1977.
10. D. R. Rutledge and A. Ostapenko, "Ultimate Strength of Longitudinally Stiffened Plate Panels (Large and Small b/t, General Material Properties) ," Fritz Engineering Laboratory Report No. 248.24, Lehigh University, 1968.
11. D. R. Rutledge, "Computer Program for Ultimate Strength of Longitudinally Stiffened Panels," Fritz Engineering Laboratory Report No. 248.23, Lehigh University, 1968.
12. S. Parsanejad and A. Ostapenko, "Ultimate Strength Analysis of Plate Grillages under Combined Loads," Fritz Engineering Laboratory Report No. 323.11, Lehigh University, 1972.
13. R. Maquoi, "Etude Theorique Et Experimentale De La Resistance Post- Critique Des Semelles Comprimees Raidies Des Ponts Metalliques En Caisson," ("Theoretical and Experimental Study of the Post- Buckling Strength of Stiffened Flanges of Steel Box Girder Bridges under Compression") (in French), Faculte des Sciences, Report No. 54, Universite de Liege, 1975.
14. M. Herzog, "Die Traglast Einseitig Langversteifter Bleche mit Imperfektionen und Eigenspannugen unter Axialdruck nach Versuchen," ("Ultimate Strength of Longitudinally Stiffened Plates According to Test Results-Consideration of Initial Imperfections and Residual Stresses") (in German), Verein Deutscher Ingenieure-Zeitung, Vol. 118, No. 7, 1976.
15. A. E. Mansour, "Charts for the Buckling and Post-Buckling Analysis of Stiffened Plates under Combined Loading," Technical and Research Bulletin No. 2-22 Society of Naval Architects and Marine Engineers, July, 1976.
16. F. Frey, "L'Analyse Statique Non Lineaire Des Structures Par La Methode Des Elements Finis Et Son Application a La Construction Metallique," ("Nonlinear Structure Analysis by the Method of Finite Elements and its Application to Steel Structures"),(in French), Faculte des Sciences, Doctoral Thesis, Universite de Liege, 1978.
17. K. Basler, "Strength of Plate Girders in Shear," Journal of the Struct. Div., ASCE, Vol. 87, No. ST7, Proc. Paper 2967, October 1961.
18. K. Basler, "Strength of plate Girders Under Combined Bending and Shear," Journal of the Struct. Div., ASCE, Vol. 87, No. ST7, Proc. Paper 2968, October 1961.
19. K. Basler and B. Thurlimann, "Strength of Plate Girders in Bending," Journal of the Struct. Div., ASCE, Vol. 87, No. ST7, Proc. Paper 2913, August 1961.
20. W. Schueller and A. Ostapenko, "Tests on a Transversely Stiffened and on a Longitudinally Stiffened Unsymmetrical Plate Girder , WRC Bulletin No. 156, November 1970.
21. A. Ostapenko and C. Chern, "Ultimate Strength of Longitudinally Stiffened Plate Girders under Combined Loads", IABSE Proceedings, Vol. 11, II, London, 1971.
22. A. Ostapenko, C. Chern, and S. Parsanejad, " Ultimate Strength Design of Plate Girders", in Developments in Bridge Design and Construction, Crosby, Lockwood and Son, Ltd., University College, Cardiff, 1971.
23. Ch. Massonnet, M. Skaloud and J. Donea, "Comportement Postcritique Des Cisaillees Raidies" ("Postbuckling Behavior of Stiffened Plates Subjected to Pure Shear"), IABSE, Proceedings, Vol. 28, II, Zurich, 1968.
24. K. C. Rockey, H.R. Evans and D. M. Porter, "A Design Method for Predicting the Collapse Behavior of Plate Girders," Proc. Institution of Civil Engineers, Part 2, Vol. 65, p. 85-112, March 1978.
25. M. Herzog, "Ultimate Strength of Plate Girders From Tests, Journal of the Struc. Div., ASCE, Vol. 100, No. ST5, Proc. Paper 10530, May 1974.

26. Ch. Massonnet, "Design of Steel Plate and Box Girder Bridges," Journal of Struc. Div., ASCE, Vol. 101, No. 11, Proc. Paper 11686, p.2477, 1975.
27. J. D. Vernarr, "Comparison Study of Plate Girder Ultimate Strength Methods," Report CE 481, Department of Civil Engineering, Lehigh University, September 1977.
28. R. Wolchuk and R. Mayrbaurl, "Proposed Design Specifications for Steel Box Girder Bridges," Report No. FHWA-TS-80-205, U.S. Federal Highway Administration, Washington, 1980.
29. J. A. Corrado, "Ultimate Strength of Single-Span, Rectangular Steel Box Girders," Ph.D. Dissertation, Fritz Engineering Laboratory Report No. 380.3, Lehigh University, University Microfilms Ann Arbor, 1971.
30. A. Ostapenko, "Shear Strength of Longitudinally Stiffened Plate Girders," Proceedings of structural Stability Research Council, 1980.
31. A. C. Walker and P. Davies, "An Elementary Study of Non-Linear Buckling Phenomena in Stiffened Plates," in Proceedings of Symposium on Structural Analysis, Non-Linear Behavior and Techniques, Transport and Road Research Laboratory (TRRL) Supplementary Report 164 UC, p. 19, 1975.
32. A. Ostapenko, "Ultimate Strength Design of Wide Stiffened Plates Loaded Axially and Normally," in Proceedings of Symposium on Structural Analysis, Non-Linear Behavior and Techniques, Transport and Road Research Laboratory (TTRL) Supplementary Report 164 UC, p. 175, 1975.
33. A. Ostapenko and A. Vaucher, "Ultimate Strength of Ship Hull Girders under Moment, Shear and Torque," MARAD Report No. MA-RD-940- 80077 (Fritz Engineering Laboratory Report No. 453.6), July 1980.
34. American Society for Testing and Materials 1971, Annual Book of ASTM Standards, Part 31, ASTM Specification E8-69, American Society for Testing and Materials, Philadelphia, Pa. 1971.